ISSN 2096-7071 (Print)
ISSN 2096-3101 (Online)
CN 10-1629/R1

CHINA CDC WEEKLY

Vol. 6 No. 35 Aug. 30, 2024

中国疾病预防控制中心周报

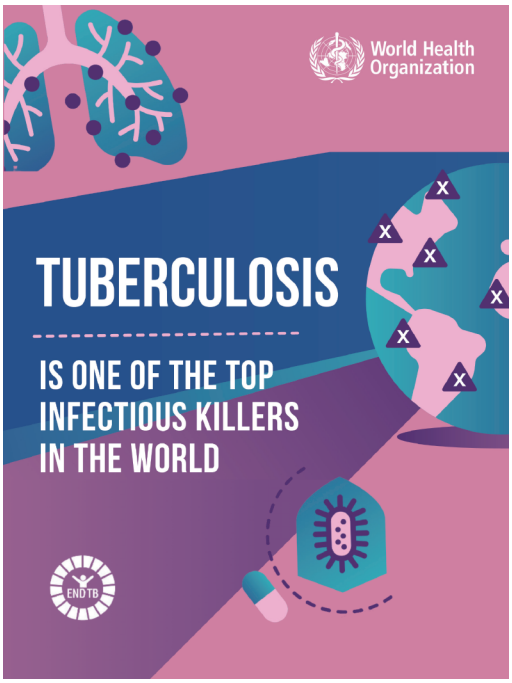

ISSN 2096-7071
9 772096 707248 35>

China CDC Weekly

Cover Image: adapted from the World Health Organization, https://www.who.int/multi-media/details/tuberculosis-is-one-of-the-top-infectious-killers-in-the-world-2023.

Preplanned Studies

A Modeling Study Recurrent Tuberculosis Towards End TB Strategy — China, 2025–2035

Tao Li[1,2,3,4]; Xin Du[2]; Zhongwei Jia[4,5,6,#]; Yanlin Zhao[2,3,#]

Summary

What is already known about this topic?

The recurrence of tuberculosis (TB) following successful treatment presents a significant challenge.

What is added by this report?

Achieving the global End TB Strategy milestones and targets with the current strategies in China is challenging. However, interventions following recovery to prevent recurrence, in conjunction with preventive treatment for latent TB infection (LTBI), will aid in meeting these objectives.

What are the implications for public health practice?

Implementing interventions to mitigate recurrence is essential for improving TB control strategies both in China and worldwide. Concurrently, the development of new drugs and vaccines should focus on preventing TB recurrence.

The global challenge of tuberculosis (TB) recurrence after successful treatment persists despite national TB programs primarily focusing on patient detection and management of treatment. These programs often overlook the need for follow-up and intervention post-treatment. Although the incidence of TB in China has been steadily declining, significant efforts are still required to achieve the END-TB targets. This study utilizes a transmission dynamic model to evaluate the impact of various control strategies on accelerating TB elimination in China. Under the current strategies, TB incidence rates in China are projected to decrease to 44.9 per 100,000 by 2030 and to 40.4 per 100,000 by 2035. Introducing post-recovery interventions to prevent recurrence, along with providing TB preventive treatment (TPT) to 30% of individuals with latent TB infection (LTBI) starting in 2025 and increasing LTBI TPT coverage to 90% beginning in 2031, will contribute to achieving the milestones of the End TB Strategy by 2030 and the 2035 target.

TB continues to pose a significant threat to public health worldwide, including in China. The World Health Organization's (WHO) End TB strategy targets a reduction in global TB incidence by 80% by 2030 and by 90% by 2035 relative to 2015 levels. In 2022, China reported an estimated 748,000 TB cases, ranking third globally with an incidence rate of 55 cases per 100,000 people. From 2000 to 2022, the annual average percentage change (AAPC) in TB incidence in China was approximately 3.1%, surpassing the global rate of 1.2% during the same timeframe (*1*). However, this progress remains substantially below the WHO's target AAPC of 10% by 2025, necessary to meet the 2030 milestone of the End TB Strategy. Although most TB patients can be effectively treated with chemical therapy, the recurrence of TB post-treatment presents a significant hurdle. In 2022, there were over 350,000 cases of recurrent TB globally, constituting 5.5% of the 6.43 million newly reported cases. This issue is particularly acute in high-burden countries such as the Russian Federation, where the rate reaches 21%. Recurrent TB often involves more complicated pathologies, increasing the risk of clinical complications and drug resistance, thereby complicating treatment and management, and exacerbating transmission risks. This study aims to develop a dynamic model to analyze TB incidence in China from 2005 to 2022 and forecast trends up to 2030 and 2035, considering both existing strategies and hypothetical scenarios with enhanced measures for recurrence control.

Recurrence was defined as the condition in which patients, previously treated and declared cured or having completed treatment for TB, are diagnosed with a subsequent episode of TB, which could either be a true relapse or a new episode caused by reinfection (*2*). TPT was defined as the administration of treatment to individuals considered at risk for developing TB disease, with the aim of reducing this risk. This is also known as LTBI treatment or preventive therapy. The WHO recommends TPT for specific target populations, including people living with human immunodeficiency virus (HIV), household contacts of bacteriologically confirmed pulmonary TB patients, and others at heightened risk

of TB such as individuals initiating antitumor necrosis factor (anti-TNF) treatment, those receiving dialysis, preparing for organ or hematological transplants, or having silicosis. Secondary preventive treatment was defined distinctly from TPT for LTBI, aimed to reduce the risk of recurrence following a successfully treated TB episode.

The compartmental model is a classical mathematical framework utilized to model the dynamics of infectious diseases. It categorizes individuals into distinct groups, with each group sharing average characteristics and typically exhibiting uniform interactions. In this study, a SEIR compartmental model was constructed to analyze the transmission dynamics of *Mycobacterium tuberculosis* (*M. tb*), incorporating the risk of recurrence based on a literature review (*3*–*4*). The simulations were conducted using the Epimodel package in R software (version 4.0.3; R Core Team, Vienna, Austria), and the model's structure is depicted in Figure 1.

The model delineates several states in the progression of TB. Susceptible (S): Individuals who have not been infected with *M. tb*. Latent Infection (E): Individuals who are infected with *M. tb* but have not developed active disease are subdivided into fast-progressing (E_{fast}) and slow-progressing (E_{slow}) categories. Previous research indicates that the lifetime risk of progressing to active TB post-infection ranges from 5%–10%, with approximately 50% developing the disease within the first 2–5 years (γ_1) and the others during subsequent periods (γ_2). Infectious (I): Active TB cases, split into newly diagnosed, untreated patients (I_n) and those with previously treated TB (I_r). Recovered (R): Individuals who have either been cured or completed their treatment regimen. The model outlines potential outcomes for TB patients: ① cure or completion of treatment (η_1, η_2), ② treatment failure (f_1, f_2), and ③ death attributed to TB (m_1, m_2) or other causes (m_0). Additionally, individuals in the recovered category (R) may suffer a recurrence (ρ), transitioning back to being infectious (I_r).

The equations of the model are as follows:

$$N(0) = S(0) + E(0) + I(0) + R(0)$$

$$m_0 + cfr + \eta + f = 1$$

$$f_1 = 1 - m_0 - cfr_1 - \eta_1$$

$$f_2 = 1 - m_0 - cfr_2 - \eta_2$$

$$\Delta S = \alpha - \beta \times (S \times I/N) - m_0 \times S$$

$$\Delta E_{fast} = (1 - g) \times \beta \times (S \times I/N) - \gamma_1 \times E_{fast} - m_0 \times E_{fast}$$

$$\Delta E_{slow} = g \times \beta \times (S \times I/N) - \gamma_2 \times E_{slow} - m_0 \times E_{slow}$$

$$\Delta I_n = \gamma_1 \times E_{fast} + \gamma_2 \times E_{slow} - I_n$$

$$\Delta I_r = f_1 \times I_n + f_2 \times I_r - \eta_2 \times I_r - (m_0 + cfr_2) \times I_r + \rho \times R$$

$$\Delta R = \eta_1 \times I_n + \eta_2 \times I_r - \rho \times R - m_0 \times R$$

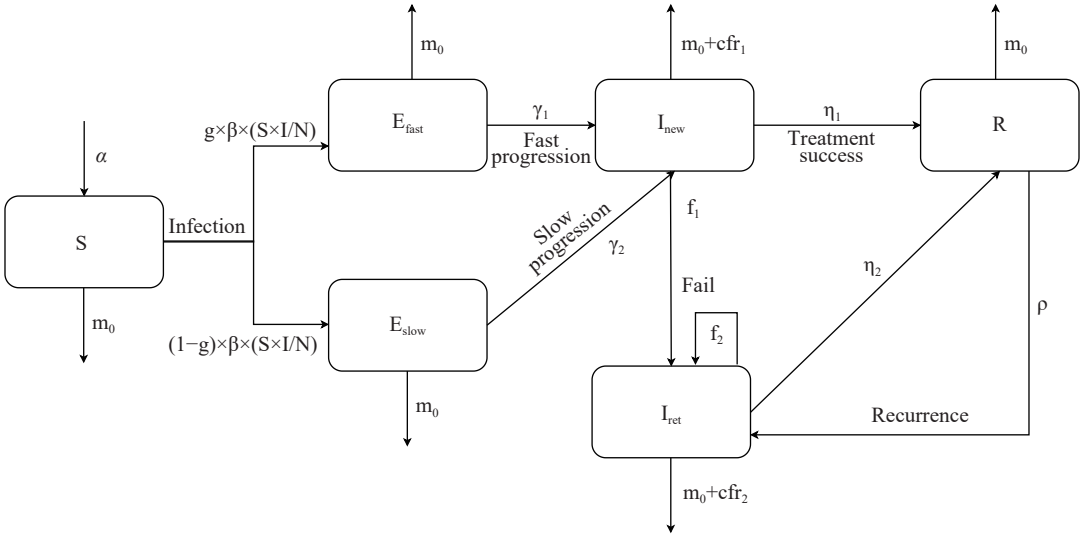

FIGURE 1. The flow diagram of TB transmission dynamic model considering recurrence.
Note: *N* refers to the total population. α is the birth rate; β is the transmission rate of infectious cases; g is the proportion of slow progression; γ is the progressive rate (divided into γ_1 and γ_2 for fast and slow progression) from latent infection to infectious; η is the proportion of successful treatment (divided into η_1 and η_2 based on treatment history); f is the proportion of treatment failure (divided into f_1 and f_2 based on treatment history); m_0 is the natural mortality rate; cfr is the fatality rate of infectious due to TB disease (divided into cfr_1 and cfr_2 based on treatment history); ρ is the recurrence rate from recovered individuals.
Abbreviation: TB=tuberculosis.

The parameters β, $\gamma 1$, and $\gamma 2$, along with the initial values for the compartments $E_{fast}(0)$ and $E_{slow}(0)$, were calibrated in the model using the optim() function, utilizing TB incidence data in China from 2013 to 2022. The aim was to minimize the root mean square error (RMSE) between the predicted and observed data. Initial values for $I_{new}(0)$, $I_{ret}(0)$, and R(0) were derived using data from the Chinese national TB surveillance system, underreporting survey, and the WHO country database. Demographic data were sourced from the China Statistical Yearbook 2023, while treatment-related parameters were computed from the national TB surveillance system. Natural history parameters were drawn from prior research (Table 1).

Six scenarios, including one baseline and five intervention scenarios to be initiated from 2025, were designed to model current and potential future TB incidence in China. Baseline Scenario: reflects current conditions without additional interventions. Scenario 2 (Recurrence-Free Treatment Scenario): projects a 90% decrease in recurrence rate through novel treatment regimens. Scenario 3 (solely Post-Treatment Intervention Scenario): incorporates an 85% reduction in recurrence risk, deploying new vaccines and secondary preventative treatments, along with follow-up for recovered TB patients. Scenario 4 (Scenario 3 + TPT for 30% LTBI): expands on Scenario 3 by including TPT for 30% of the LTBI population starting in 2025 to expedite progress toward the 2030 End TB strategy milestone. The efficacy of TPT in reducing TB risk among the LTBI population is estimated at 90%. Scenario 5 (Control against Scenario 4): focuses on the LTBI intervention alone as a comparison to Scenario 4 with an identical outcome, increasing TPT coverage to 50% of the LTBI population. Scenario 6 (Scenario 4 + Enhanced TPT for 90% of the LTBI Population Beginning in 2031):

TABLE 1. Estimated values of parameters and initial compartments.

Parameter/compartment	Definition	Estimated value	Resource
α	Birth rate	Annual birth rates during 2005–2022 (‰)	China Statistical Yearbook (*5*)
m_0	Natural mortality rate	Annual natural mortality rates during 2005–2022 (‰)	China Statistical Yearbook (*5*)
g	Proportion of individuals with slow progression among latent infections	91%	Ragonnet et al. (*3*)
η_1	Successful treatment rate for new patients	94%	National TB surveillance system
η_2	Successful treatment rate for retreated patients	85%	National TB surveillance system
cfr_1	Case fatality rate for new patients	3%	Straetemans et al. (*6*)
cfr_1	Case fatality rate for retreated patients	9%	Straetemans et al. (*6*); Mathew et al. (*7*)
β	Transmission rate	2.35	Model fitting
γ_1	Progressive rate for slow progression LTBI	0.038	Model fitting
γ_2	Progressive rate for fast progression LTBI	0.00046	Model fitting
ρ	Recurrence rate for recovered patients	0.0005	National TB surveillance system
$N(0)$	General population in 2013	1,367,260,000	China Statistical Yearbook (*5*)
$S(0)$	Susceptible patients in 2013	1,104,396,330	N(0)-E(0)-I(0)-R(0)
$E(0)$	LTBI in 2013	247,200,608	Gao et al. (*8*)
$E_{fast}(0)$	Fast progression among LTBI in 2013	20,996,170	Model fitting
$E_{slow}(0)$	Slow progression among LTBI in 2013	226,204,438	Model fitting
$I_{new}(0)$	Newly diagnosed TB patients	884,206	Chinese national TB surveillance system/ underreporting survey/ WHO country database
$I_{ret}(0)$	Previously treated TB patients	81,097	Chinese national TB surveillance system/ underreporting survey/ WHO country database
$R(0)$	Recovered	14,558,870	Chinese national TB surveillance system/ underreporting survey/ WHO country database

Abbreviation: WHO=World Health Organization; TB=tuberculosis; LTBI=latent tuberculosis infection.

Extends Scenario 4 by raising the TPT coverage for the LTBI population to 90% starting in 2031, accelerating achievement of the 2035 End TB strategy goals.

RESULTS

Under the baseline scenario, it is anticipated that the incidence of TB in China will decrease to 44.9 per 100,000 by 2030 and further to 40.4 per 100,000 by 2035. Should a new "recurrence-free" regimen be introduced from 2025 (Scenario 2), the incidence is expected to drop to 43.6 per 100,000 by 2030, indicating a 2.9% additional reduction compared to the baseline. Implementing post-recovery interventions for all recovered TB patients (Scenario 3) could lead to an incidence rate of 38.3 per 100,000 by 2030, marking a 14.7% greater decline relative to the baseline. Introducing TPT for 30% of LTBI cases in addition to Scenario 3 measures (Scenario 4) could further lower the incidence to 29.2 per 100,000 by 2030, thus meeting the 2030 End TB Strategy milestone of less than 30 per 100,000 with a 35.0% greater reduction compared to the baseline. Implementing TPT alone for 50% of LTBI cases (Scenario 5) could reduce the incidence to 28.8 per 100,000 by 2030. Scenario 4 would require a total of 98.5 million recovered patients and LTBI cases to receive preventive treatment, while Scenario 5 would entail treatment for 123.8 million LTBI cases. Scenario 4 could result in cost savings of 4.6 to 7.9 billion Chinese Yuan (CNY) over Scenario 5 by reducing the number of treatment recipients by 25.4 million, assuming treatment costs between 180–310 CNY per person for a 6-month course of isoniazid (6H) or a 3-month regimen of isoniazid combined with rifampentine (3HP). Extending the coverage of LTBI preventive treatment to 90% beyond 2030 as per Scenario 4 could reduce the incidence to 9.7 per 100,000 by 2035, thereby achieving the 2035 End TB Strategy goal of less than 10 per 100,000 (Figure 2).

DISCUSSION

The TB incidence rate in China showed a continuous downward trend. However, it is difficult to achieve the global End TB Strategy milestone and target with the current strategies. Implementing post-recovery interventions combined with 30% LTBI TPT

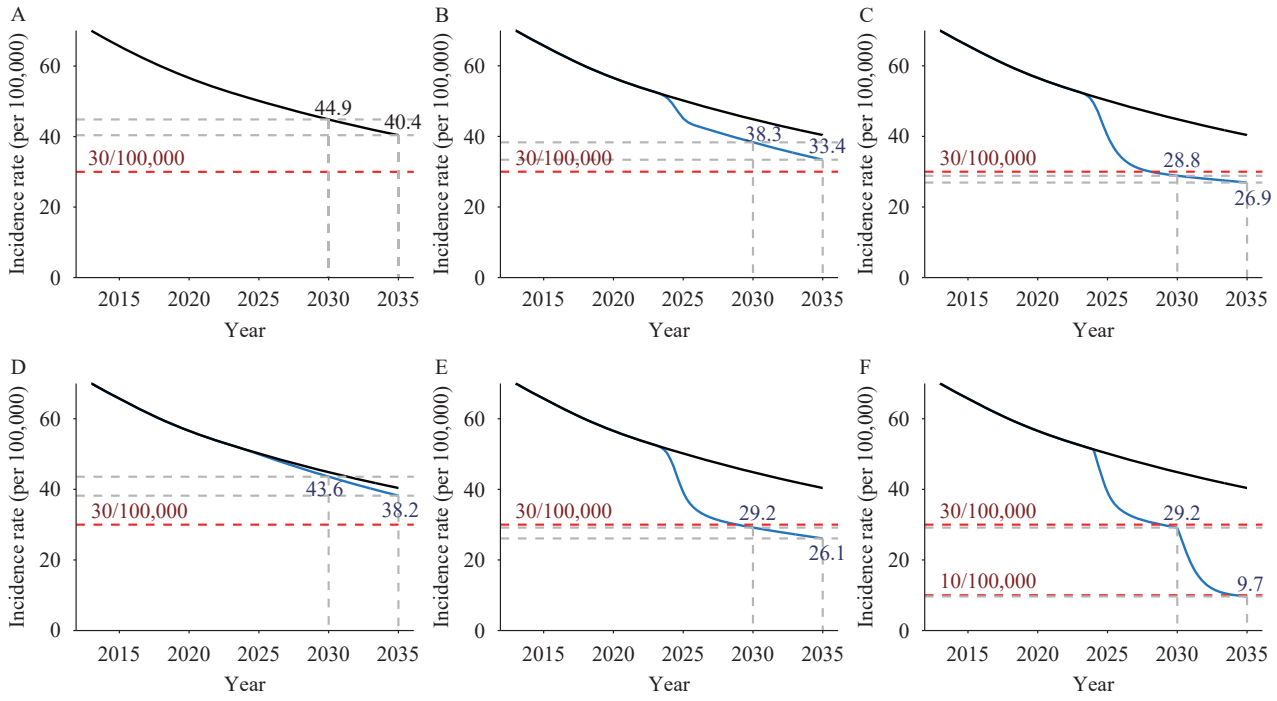

FIGURE 2. Predictions of TB incidence in China with different interventions, 2013–2035. (A) Baseline scenario; (B) Scenario 2 − Recurrence free treatment scenario; (C) Scenario 3 − Sole Post − Treatment Intervention Scenario; (D) Scenario 4 − Scenario 3 + TPT for 30% LTBI; (E) Scenario 5 − Control scenario against scenario 4; (F) Scenario 6 − Scenario 4 + TPT for 90% LTBI since 2031.
Abbreviation: TB=tuberculosis; TPT=tuberculosis preventive treatment; LTBI=latent tuberculosis infection.

from 2025 and expanding LTBI TPT coverage to 90% from 2031 will help achieve these goals.

Patients with TB exhibit a recurrence risk significantly higher than the incidence risk in the general population. Studies indicate that the recurrence rate in Shanghai Municipality is more than 18 times the local incidence rate. Reducing recurrence is crucial for assessing the clinical outcomes of novel TB vaccines and treatments. Recent clinical trials have tested several vaccines, and studies on treatment regimens that incorporate new second-line anti-TB drugs, such as Bedaquiline, Delamanid, and Pretomanid, have demonstrated reduced recurrence rates in rifampin-resistant patients. Moreover, nursing interventions, including psychological support, health education, and dietary guidance, have been effective in improving treatment adherence and potentially reducing recurrence rates. However, enhancing treatment regimens, whether through new drugs, improved patient care, or combination with therapeutic vaccines, falls short of achieving the milestones set for the 2030 End TB Strategy (Scenario 2). These strategies primarily benefit newly diagnosed patients and fail to address the needs of a large number of previously treated patients who remain at high risk for recurrence.

Following up with TB patients post successful treatment is crucial for early detection of recurrence and for mitigating risk. Secondary preventive treatment with isoniazid has been shown to effectively reduce TB recurrence (*9*). Previous modeling studies have demonstrated that screening for LTBI and administering preventive treatment can rapidly decrease TB incidence (*10*). However, widespread screening in the general population is hampered by high costs and low acceptance of the TPT, particularly impeding global TPT progress, notably in China. Acceptance of secondary preventive treatment may be higher among previously treated TB patients due to their familiarity with the disease. This modeling study indicates that strategies to prevent recurrence in all previously treated TB patients — through routine follow-up, secondary preventive treatment, and potential re-vaccination — could significantly hasten the reduction of TB incidence. Despite these interventions, the 2030 milestone (Scenario 3) remains unachievable. When these strategies are accompanied by TPT for 30% of individuals with LTBI (Scenario 4), achieving the 2030 milestone is feasible. By contrast, without recurrence intervention, TPT would need to extend to 50% of infected individuals (Scenario 5) to accomplish the same outcome, significantly raising both costs and implementation challenges. Although Scenario 4 can meet the 2030 End TB milestone, it falls short of the 2035 target. Only by expanding TPT to 90% of individuals with LTBI (Scenario 6), a largely impractical goal, can the 2035 target potentially be met.

The study was subject to some limitations. First, the underlying causes of TB recurrence may include endogenous reactivation or exogenous reinfection, and the effectiveness of various recurrence control interventions may differ across settings with varying TB burdens. Additionally, other effective interventions, such as active case finding, can also accelerate the reduction in TB incidence rates. Future efforts to implement recurrence interventions should be tailored to specific local conditions. Second, the efficacy of secondary preventive treatment with isoniazid has only been confirmed in HIV-positive TB patients. We hypothesize that it is equally effective in HIV-negative TB patients, similar to those without a treatment history, but this assumption requires further validation in future studies. Finally, our model did not distinguish between different types of TB (pulmonary or extrapulmonary). Nevertheless, the transmission rates, which are critical for influencing the outcomes, were derived through model fitting. Moreover, the parameters sourced from the surveillance system encompassed data from all TB forms. Hence, our results inherently represent a blended effect of both pulmonary and extrapulmonary TB.

According to estimates by Dodd et al. (*11*), there were approximately 155 million TB survivors worldwide in 2020. Recurrence presents a significant obstacle to achieving the global objective of TB elimination. National TB programs predominantly emphasize patient detection and treatment management, while often neglecting post-treatment follow-up and interventions. Implementing strategies to reduce recurrence is critical for improving TB control efforts both in China and around the world. Additionally, the development of new drugs and vaccines should focus on preventing recurrence and expedite the assessment of these innovations.

Conflicts of interest: No conflicts of interest reported.

Funding: Supported by the project "Epidemic of Tuberculosis Recurrence and Types of Recent Recurrence in Western China" (JY22-3-11), the Chinese Center for Disease Control and Prevention, and the National Natural Science Foundation of China (72174004).

doi: 10.46234/ccdcw2024.189

[#] Corresponding authors: Zhongwei Jia, urchinjj@163.com; Yanlin Zhao, zhaoyl@chinacdc.cn.

[1] Department of Epidemiology and Biostatistics, School of Public Health, Peking University, Beijing, China; [2] Chinese Center for Disease Control and Prevention, Beijing, China; [3] National Key Laboratory of Intelligent Tracking and Forecasting for Infectious Diseases, Chinese Center for Disease Control and Prevention, Beijing, China; [4] Center for Intelligent Public Health, Institute for Artificial Intelligence, Peking University, Beijing, China; [5] Department of Global Health, School of Public Health, Peking University, Beijing, China; [6] Center for Drug Abuse Control and Prevention, National Institute of Health Data Science, Peking University, Beijing, China.

Submitted: February 21, 2024; Accepted: August 01, 2024

REFERENCES

1. World Health Organitation. Global tuberculosis report 2023. Geneva: World Health Organitation; 2023. https://digitallibrary.un.org/record/4026851?ln=zh_CN.
2. World Health Organization. Definitions and reporting framework for tuberculosis – 2013 revision: updated December 2014 and January 2020. Geneva: World Health Organization; 2013. https://iris.who.int/handle/10665/79199.
3. Ragonnet R, Trauer JM, Scott N, Meehan MT, Denholm JT, McBryde ES. Optimally capturing latency dynamics in models of tuberculosis transmission. Epidemics 2017;21:39 – 47. https://doi.org/10.1016/j.epidem.2017.06.002.
4. Philippe G, Charalambos S, Carel P, Katherine F. Methods used by WHO to estimate the Global burden of TB disease. 2016. http://arxiv.org/abs/1603.00278. [2024-2-1].
5. National Bureau of Statistics of China. China statistical yearbook 2023. Beijing: China Statistics Press. 2023. https://book.kongfz.com/446662/7079358823. (In Chinese)
6. Straetemans M, Glaziou P, Bierrenbach AL, Sismanidis C, van der Werf MJ. Assessing tuberculosis case fatality ratio: a meta-analysis. PLoS One 2011;6(6):e20755. https://doi.org/10.1371/journal.pone.0020755.
7. Mathew TA, Ovsyanikova TN, Shin SS, Gelmanova I, Balbuena DA, Atwood S, et al. Causes of death during tuberculosis treatment in Tomsk Oblast, Russia. Int J Tuberc Lung Dis 2006;10(8):857-63. https://www.ingentaconnect.com/content/iuatld/ijtld/2006/00000010/00000008/art00007;jsessionid=4bi47owb3ppcu.x-ic-live-01.
8. Gao L, Zhang H, Hu MG, Xu CD, Xia YY, Li T, et al. Estimation of the national burden on latent tuberculosis infection based a multi-center epidemiological survey and the space statistics model. Chin J Antituberc 2022;44(1):54 – 9. https://doi.org/10.19982/j.issn.1000-6621.20210661.
9. Fitzgerald DW, Desvarieux M, Severe P, Joseph P, Johnson WD, Pape JW. Effect of post-treatment isoniazid on prevention of recurrent tuberculosis in HIV-1-infected individuals: a randomised trial. Lancet 2000;356(9240):1470 – 4. https://doi.org/10.1016/S0140-6736(00)02870-1.
10. Houben RMGJ, Menzies NA, Sumner T, Huynh GH, Arinaminpathy N, Goldhaber-Fiebert JD, et al. Feasibility of achieving the 2025 WHO global tuberculosis targets in South Africa, China, and India: a combined analysis of 11 mathematical models. Lancet Glob Health 2016;4(11):e806 – 15. https://doi.org/10.1016/S2214-109X(16)30199-1.
11. Dodd PJ, Yuen CM, Jayasooriya SM, van der Zalm MM, Seddon JA. Quantifying the global number of tuberculosis survivors: a modelling study. Lancet Infect Dis 2021;21(7):984 – 92. https://doi.org/10.1016/S1473-3099(20)30919-1.

Preplanned Studies

Effectiveness of C-Reactive Protein as a Tuberculosis Screening Test Among HIV-Infected Individuals — Shanghai, China, 2021–2023

Lixin Rao[1]; Zheyuan Wu[1]; Jing Chen[1]; Zhen Ning[1]; Xin Shen[1,#]

Summary

What is already known about this topic?

The World Health Organization (WHO) has recommended the inclusion of the C-reactive protein (CRP) test in active tuberculosis (ATB) screening algorithms among human immunodeficiency virus (HIV)-infected individuals. The performance of the CRP test in African regions has been well-documented.

What is added by this report?

This study analyzed data from a big data platform of Shanghai medical records together with infectious disease surveillance systems. We simulated a screening and plotted a receiver operating characteristic (ROC) curve, which gives the optimal cut-off value of 11.115mg/L with sensitivity and specificity of 0.784 and 0.723, respectively.

What are the implications for public health practice?

We obtained a promising perspective on screening for tuberculosis in people living with HIV (PLHIV) using the CRP test in Shanghai. Our study offers an original standpoint for following research.

Co-infection with *Mycobacterium tuberculosis* (MTB) and human immunodeficiency virus (HIV) has emerged as a growing global concern. HIV-positive cases accounted for 6.3% of incident cases and 14.8% of deaths among all tuberculosis (TB) cases in 2022 (*1*). The World Health Organization (WHO) has recommended the inclusion of the C-reactive protein (CRP) test in the active tuberculosis (ATB) screening algorithm in its latest guidelines (*2*). CRP is a non-specific inflammatory biomarker that rises when the body encounters interleukin-6-induced pyogenic infection (such as TB). Research shows that the CRP test has similar sensitivity to, and better specificity than, WHO-recommended four-symptom screening (W4SS) among people living with HIV (PLHIV) in all sub-populations. With a negative predictive value of 97.3%, the CRP test is an ideal rule-out exam to reduce the number of individuals who need further confirming tests by 36%, thus saving a large amount of health resources (*2–3*). The performance of the CRP test in African regions has been well-documented (*4*). However, the suitability and effectiveness of the CRP test in low HIV burden and moderate TB burden regions, such as Shanghai Municipality, China, are currently unknown. This study utilized health service data from all health facilities in Shanghai, along with patient management data of infectious diseases, to assess the use of the CRP test and calculate the sensitivity and specificity of CRP results in relation to TB screening. Propensity score matching (PSM) was employed to match HIV-infected and HIV-uninfected tuberculosis patients. A receiver operating characteristic (ROC) curve was plotted, and the area under the curve (AUC), optimal sensitivity, and specificity were determined. Among included participants, 94 TB/HIV patients, 986 HIV-negative TB patients, and 282 PLHIV (excluding TB) were matched to at least one CRP test record. We simulated TB screening and plotted the ROC curve, with AUC values of 0.616 for the entire study population and 0.801 for PLHIV only. The best CRP threshold for PLHIV is 11.115 mg/L. Our study offers a promising opportunity to screen for tuberculosis among PLHIV using the CRP test in Shanghai.

In this study, patient information was collected for individuals with active pulmonary tuberculosis and PLHIV from the China Information System for Disease Control and Prevention (CISDCP). The ATB patients were diagnosed between January 1, 2018 and October 31, 2023, according to the National Industry Standard (WS 196-2017). Individuals with non-tuberculous mycobacteria and old tuberculosis lesions were excluded. PLHIV individuals were included if they were diagnosed and under surveillance before October 31, 2023. The CRP test results were extracted from the Survey System of Health Resources and Medical Services (SSHRMS) database that were associated with ATB and PLHIV individuals using a

unique identification code. The test results were collected from 100 days before to 30 days after the date of diagnosis for ATB patients and from January 1, 2021 to October 31, 2023, for PLHIV. In cases where an individual had multiple CRP test results, the record closest to the date of TB treatment for ATB patients or the latest result for PLHIV was included in the analysis.

Microsoft Excel (version 2010, Microsoft Corporation, Redmond, United States) was used for data preprocessing, including converting character variables to numerical variables, data extraction, and grouping. R (version 4.3.1, R Foundation for Statistical Computing, Vienna, Austria) was used to conduct all statistical analyses. PSM was used to match HIV-infected and non-infected tuberculosis patients at a proportion of 1:10 to control for confounding factors such as gender and age. Propensity score is a mathematical method to reduce selection bias by balancing covariates between treatment and control groups. The caliper value of the PSM was set to 0.01. A rank sum test of multiple groups of independent nonparametric samples was performed, and the Baumgartner-Wei-Schindler test was used for pairwise comparisons between groups. A receiver operating characteristic (ROC) curve was plotted, and the area under curve (AUC), optimal sensitivity, and specificity were calculated. A $P<0.05$ was considered statistically significant in all analyses.

A total of 153 TB/HIV co-morbid patients were diagnosed between January 1, 2018 and October 31, 2023. These patients were matched with 1,530 non-HIV-infected TB patients using PSM, forming one group. Another group, serving as the control, consisted of 1,033 PLHIV individuals without ATB or TB history. Before PSM, the raw treatment and control groups differed substantially (Figures 1A and 1B). After PSM, however, homogeneity improved significantly among the study groups (Figures 1C and 1D).

A total of 3,560 test records were successfully extracted according to the extraction rules described above. After matching these records with the included population, 94 of 153 TB/HIV patients, 986 of 1,530 HIV-negative TB patients, and 282 of 1,033 PLHIV (excluding tuberculosis) were found to have at least one CRP test record (Table 1).

CRP results were recoded based on actual test values

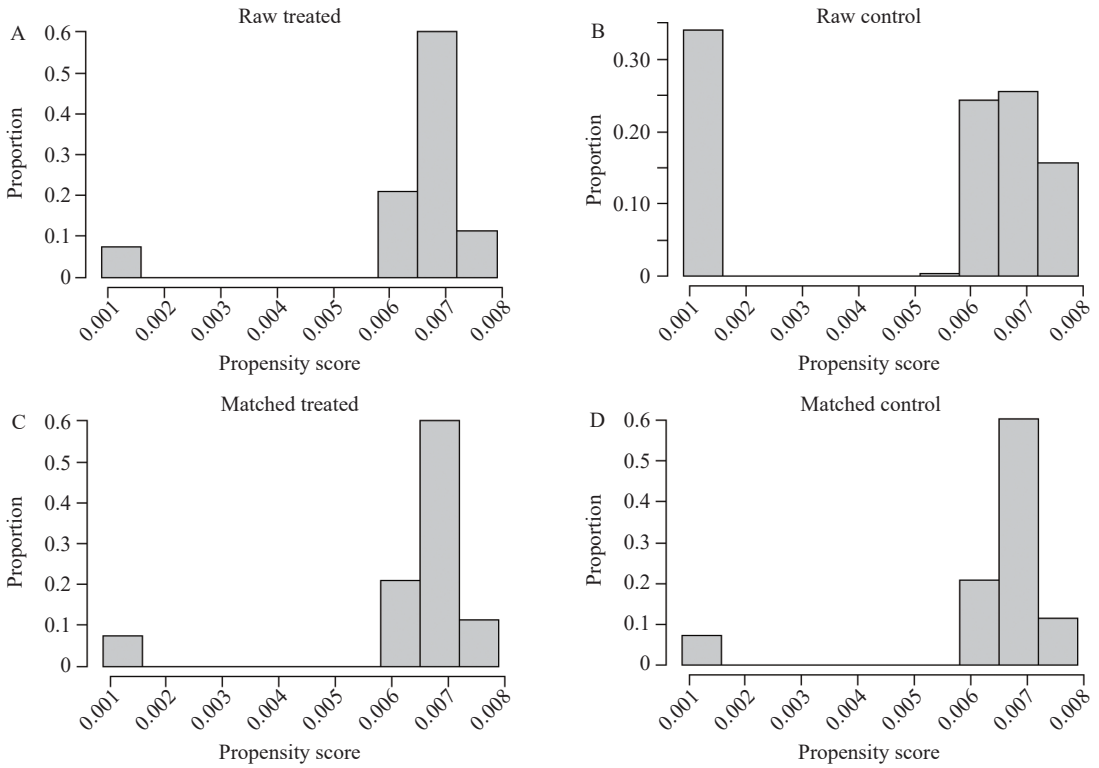

FIGURE 1. Comparison of propensity scores between TB/HIV and HIV-negative TB patients before and after PSM in Shanghai Municipality, China, 2021–2023. (A) TB/HIV before PSM; (B) HIV-negative TB patients before PSM; (C) TB/HIV after PSM; (D) HIV-negative TB patients after PSM.
Abbreviation: TB=tuberculosis; HIV=human immunodeficiency virus; PSM=propensity score matching.

TABLE 1. General characteristics of all participants with CRP results, Shanghai Municipality, China, 2021–2023.

Group	TGroupB/HIV, *N*=94	HIV-TB (after PSM), *N*=986	PLHIV (non-TB), *N*=282
Gender			
Male	90	908	261
Female	4	78	21
Age group (years)			
20–29	13	94	47
30–39	18	198	109
40–49	23	235	43
50–59	20	238	37
60–69	15	163	34
70–79	5	58	12

Abbreviation: TB=tuberculosis; HIV=human immunodeficiency virus; PLHIV=people living with HIV; CRP=C-reactive protein; PSM=propensity score matching.

TABLE 2. Count and mean of CRP results by >5 mg/L and >10 mg/L cut-off value, Shanghai Municipality, China, 2021–2023.

Group	TB/HIV	HIV-TB (after PSM)	PLHIV (non-TB)	*P*
CRP >5 mg/L				
Positive count (*N*, %)	76, 80.9	519, 52.6	117, 41.5	<0.001
Mean positive CRP	57.2	46.5	24.8	
Negative count (*N*, %)	18, 19.2	467, 47.4	165, 58.5	
Mean negative CRP	2.2	1.6	1.7	
CRP >10 mg/L				
Positive count (*N*, %)	68, 72.3	420, 42.6	63, 22.3	<0.001
Mean positive CRP	63.0	55.7	39.4	
Negative count (*N*, %)	26, 27.7	566, 57.4	219, 77.7	
Mean negative CRP	3.9	2.6	3.2	

Abbreviation: TB=tuberculosis; HIV=human immunodeficiency virus; PLHIV=people living with HIV; CRP=C-reactive protein; PSM=propensity score matching.

using cutoff values of >5 mg/L and >10 mg/L. Results for different cutoff values are presented in Table 2.

Using CRP results, we conducted TB screening among PLHIV and plotted the ROC curve (Figure 2). The AUC was 0.616 for the entire study population and 0.801 for PLHIV. The difference was statistically significant (P<0.001). Based on the ROC curve, the optimal CRP threshold for PLHIV was 11.115.

For PLHIV, at a CRP threshold of >5 mg/L, the sensitivity was 80.85% and the specificity was 58.51%. At a CRP threshold of >10 mg/L, the sensitivity was 72.23% and the specificity was 77.66%. For all participants, the sensitivity decreased to 55.09% (CRP>5 mg/L) and 45.19% (CRP>10 mg/L), while the specificity remained unchanged.

DISCUSSION

This study represents the first exploration of the feasibility and effectiveness of using CRP testing for TB screening among PLHIV in Shanghai. This study utilized resources from a big data platform, cross-matching data from the CISDCP. Because the proportion of TB/HIV co-infected individuals among all TB patients in Shanghai was relatively small, and significant differences in population characteristics were observed, PSM was employed to match individuals with similar characteristics from the entire TB patient population. Matching was based on significant TB/HIV population characteristics, such as gender and age, to minimize potential confounding factors between study groups. Following PSM, the demographic characteristics of the study population were fairly homogeneous.

After PSM, 153 patients had both TB and HIV, 1,530 patients had only TB, and 1,033 patients had only HIV. However, the proportion of cases with matching CRP results from the big data platform was

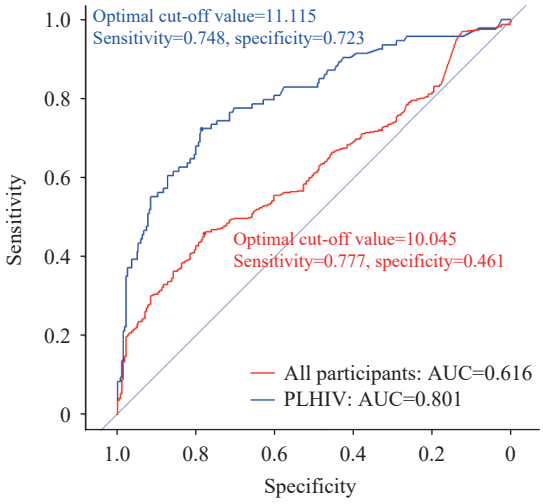

FIGURE 2. ROC curve of CRP screening for TB in all participants and PLHIV only, Shanghai Municipality, China, 2021–2023.
Abbreviation: ROC=receiver operating characteristic; CRP=C-reactive protein; TB=tuberculosis; HIV=human immunodeficiency virus; PLHIV=people living with HIV.

low: 64.17% (1,080/1,683) among active tuberculosis patients and only 31.70% (376/1,186) among HIV-positive patients. This indicates that CRP testing is not routinely used in the diagnosis and treatment of tuberculosis patients or in the follow-up examinations of HIV patients. Furthermore, our study found that of the 3,560 CRP results extracted, only 12 used POCT, accounting for a mere 0.3% of the total results. Although the WHO recommends the use of POCT-based CRP tests as a screening tool for TB in PLHIV, our findings indicate that its application is quite limited. The practical difficulties are that, in current medical facilities in Shanghai, CRP tests typically require whole blood or serum samples, professional technicians, laboratory equipment, and higher costs, restricting its use as a screening tool.

We collected original CRP results from medical facilities and classified them by cutoff values of 5 mg/L and 10 mg/L, following WHO recommendations, to compare CRP level differences among TB/HIV patients, HIV-negative TB patients, and HIV-positive individuals without ATB. Both the positive rate and mean CRP result in TB/HIV patients were the highest, with significant differences compared to the other two groups under both cutoff values. We also simulated TB screening using CRP and drew the ROC curve. CRP's effect was significantly better in PLHIV than in the general population, indicating that CRP testing is more suitable for TB screening in PLHIV. This is consistent with Meyer et al.'s conclusion (*5*). According to our data, the best CRP cutoff value for PLHIV is 11.115, with 72.23% sensitivity and 77.66% specificity. Lowering the cutoff to the WHO-recommended 5 mg/L for TB screening increases sensitivity to 80.85% but decreases specificity to 58.51%. Our results are similar to studies in India (optimal cutoff: 8.25 mg/L, sensitivity: 70.13%, specificity: 69.86) (*6*), Durban (cutoff: >10 mg/L, sensitivity: 78.6%, specificity: 72.3%) (*7*), and Kampala (cutoff: ≥10 mg/L, sensitivity: 73%, specificity: 80%) (*8*). Some studies show better results (*4*,*9*–*10*), with sensitivity reaching the WHO standard for an ideal screening tool (90%), but almost none meet the specificity standard (70%).

Finally, we must emphasize that our data were collected based on existing medical behaviors that probably were not originally intended for TB screening. Also, as a nonspecific index, CRP levels could be elevated by other concomitant infections or acute responses. Therefore, our results can only be considered an indication of the potential use of CRP as a TB screening tool among PLHIV, rather than a quantitative measure of CRP levels. This represents a significant limitation of our study, which warrants further research.

In conclusion, this study provides a promising approach to screening for TB in PLHIV using a simple blood index in this city with a population of over 30 million permanent residents. Any public health decision, no matter how small, requires significant societal resources multiplied by this population size. This study offers an original standpoint for future research to explore the method, process, algorithm, optimal screening threshold, health economic evaluation, and other details.

Conflicts of interest: No conflicts of interest.

Acknowledgements: Shanghai Municipal Health Statistics Center for their supportive contribution to this study.

Funding: Supported by the Shanghai three-year (2023–2025) action plan to strengthen the public health system (GWVI-11.1-05), the Top Young Talents in Shanghai.

doi: 10.46234/ccdcw2024.190

Corresponding author: Xin Shen, shenxin@scdc.sh.cn.

[1] Shanghai Municipal Center for Disease Control and Prevention, Shanghai, China.

Submitted: November 29, 2023; Accepted: June 18, 2024

REFERENCES

1. World Health Organization. Global tuberculosis report 2023. Geneva: World Health Organization; 2023. https://www.who.int/publications/i/item/9789240083851.
2. World Health Organization. WHO consolidated guidelines on tuberculosis: module 2: screening: systematic screening for tuberculosis disease. Geneva: World Health Organization; 2021. https://www.who.int/publications/i/item/9789240022676.
3. Dhana A, Gupta RK, Hamada Y, Kengne AP, Kerkhoff AD, Yoon C, et al. Clinical utility of WHO-recommended screening tools and development and validation of novel clinical prediction models for pulmonary tuberculosis screening among outpatients living with HIV: an individual participant data meta-analysis. Eur Respir Rev 2023;32(168):230021. https://doi.org/10.1183/16000617.0021-2023.
4. Yoon C, Chaisson LH, Patel SM, Allen IE, Drain PK, Wilson D, et al. Diagnostic accuracy of C-reactive protein for active pulmonary tuberculosis: a meta-analysis. Int J Tuberc Lung Dis 2017;21(9):1013 – 9. https://doi.org/10.5588/ijtld.17.0078.
5. Meyer AJ, Ochom E, Turimumahoro P, Byanyima P, Sanyu I, Lalitha R, et al. C-reactive protein testing for active tuberculosis among inpatients without HIV in Uganda: a diagnostic accuracy study. J Clin Microbiol 2020;59(1):e02162 – 20. https://doi.org/10.1128/JCM.02162-20.
6. Saripalli A, Ramapuram J. C-reactive protein as a screening test for tuberculosis in people living with HIV in southern India: a cross-sectional, observational study. J Clin Med 2022;11(13):3566. https://doi.org/10.3390/jcm11133566.
7. Shapiro AE, Hong T, Govere S, Thulare H, Moosa MY, Dorasamy A, et al. C-reactive protein as a screening test for HIV-associated pulmonary tuberculosis prior to antiretroviral therapy in South Africa. AIDS 2018;32(13):1811. https://doi.org/10.1097/QAD.0000000000001902.
8. Yoon C, Semitala FC, Atuhumuza E, Katende J, Mwebe S, Asege L, et al. Point-of-care C-reactive protein-based tuberculosis screening for people living with HIV: a diagnostic accuracy study. Lancet Infect Dis 2017;17(12):1285 – 92. https://doi.org/10.1016/S1473-3099(17)30488-7.
9. Calderwood CJ, Reeve BWP, Mann T, Palmer Z, Nyawo G, Mishra H, et al. Clinical utility of C-reactive protein-based triage for presumptive pulmonary tuberculosis in South African adults. J Infect 2023;86(1):24 – 32. https://doi.org/10.1016/j.jinf.2022.10.041.
10. Kagujje M, Mwanza W, Somwe P, Chilukutu L, Creswell J, Muyoyeta M. Sensitivity and specificity of CRP and symptom screening as tuberculosis screening tools among HIV-positive and negative outpatients at a primary healthcare facility in Lusaka, Zambia: a prospective cross-sectional study. BMJ Open 2023;13(4):e061907. https://doi.org/10.1136/bmjopen-2022-061907.

Methods and Applications

Evaluation of Latent Tuberculosis Infection Using the ESAT6-CFP10 Skin Test Among International Freshmen With Diverse Skin Tones at a University — Nanjing City, Jiangsu Province, China, September 2023

Peng Lu[1,2,&]; Rong Wang[3,&]; Jingjing Xu[2]; Jianming Wang[2]; Fangfang Du[4]; Guozhi Wang[5]; Shiming Cheng[4,#]; Limei Zhu[1,#]

ABSTRACT

Introduction: Newer skin tests, including the ESAT6-CFP10 (EC) skin test, were recommended for diagnosing *Mycobacterium tuberculosis* (*M. tb*) infection. However, no data exist assessing the diagnostic performance of the EC skin test among foreign students with different skin tones.

Methods: A cohort study at Nanjing Medical University screened incoming foreign freshmen. The EC skin test was used to assess for *M. tb* infection, and results were read at 24, 48, 72, and 96-hours post-administration.

Results: Among 96 participants, *M. tb* infection rates at 24, 48, 72, and 96-hours post-injection were 3.13%, 7.29%, 13.54%, and 9.38%, respectively. While infection rates were lower among individuals with darker skin tones, the difference was not statistically significant (P=0.186), and variations were consistent across different measurement times. Trajectory analysis revealed 5.3% in the continuous-increasing group, 86.5% in the low-stable group, and 5.2% in the elevated-decreasing group. Notably, participants in the elevated-decreasing group had lighter skin tones, with trajectory patterns consistent across different skin colors.

Discussion: The EC skin test is safe, and redness diameter is a more reliable indicator than induration. Results should be collected within 48 to 72 hours, with verification at 72 hours crucial if initial results are negative. Importantly, skin color does not affect EC skin test outcomes.

Globally, an estimated 7.5 million new tuberculosis cases were reported in 2022, with 87% concentrated in 30 high-burden countries. Approximately one-fourth of the global population is infected with *Mycobacterium tuberculosis* (*M. tb*) (*1*). The World Health Organization (WHO) guidelines strongly recommend screening and treatment for *M. tb* infection in populations at high risk for tuberculosis. Such screening is also conditionally recommended for recent immigrants from high-incidence to low-incidence settings (*2*). Identifying specific immigrant groups, such as foreign students, for *M. tb* infection management remains challenging in China. Tuberculosis outbreaks in schools have been frequently reported in recent years, partly due to inadequate tuberculosis screening of incoming freshmen (*3*). The prevalence of *M. tb* infection among freshmen in China, as determined by various diagnostic tests, ranged from 1% to 25% (*3*–*4*).

In 2022, alternative methods for diagnosing *M. tb* infection, including newer skin tests based on *M. tb* antigens, were recommended. One such test is the ESAT6-CFP10 (EC) skin test (*5*). Recent studies have indicated that the EC skin test demonstrates comparable diagnostic efficacy to IGRAs in the general population (*6*). Unlike Cy-Tb and Diaskintest, which measure induration diameters, the EC skin test uses the larger measurement of either induration or redness reaction. Redness has been shown to be clearly visible and measurable in Chinese individuals with lighter skin tones (*7*). However, whether the redness reaction of the EC skin test can be accurately measured on darker skin tones remains uncertain. Furthermore, data evaluating the diagnostic performance of the EC skin test among foreign students with varying skin tones are lacking.

To address this question, we recruited foreign students at Nanjing Medical University to assess the performance of the EC skin test in this high-risk population.

METHOD

Study Design and Participants

This cohort study was conducted in September 2023 at Nanjing Medical University. Screening was conducted as part of the admission process for foreign students in Jiangsu Province. Foreign students are required to undergo *M. tb* infection screening before university enrollment. The EC skin test developed by Zhifei Longcom Biologic Pharmacy Company was used to assess *M. tb* infection. Individuals were excluded if they had acute infectious diseases (e.g., measles, pertussis, influenza, pneumonia), acute conjunctivitis, or acute otitis media; a history of multiple drug allergies; or a history of hysteria.

Procedures

For eligible participants, demographic information, including name, gender, age, nationality, educational background, and history of tuberculosis exposure, was collected before EC skin testing. EC skin tests were performed using the Mantoux method on the volar surface of the left forearm (*7*). Chest X-ray images were taken for all individuals before EC testing to rule out tuberculosis. Subsequently, EC skin test results were assessed at 24, 48, 72, and 96-hours post-administration. At each time point, induration and redness diameters were recorded, and images were captured to verify reactions. Each participant was monitored for a minimum of 30 minutes following test administration to detect acute adverse reactions. Pictures of induration and redness diameters were collected and examined by different staff members. Individuals were excluded from the study if they had acute infectious diseases (e.g., measles, whooping cough, influenza, pneumonia), acute conjunctivitis, or acute otitis media; a history of multiple drug allergies or hysteria; systemic skin diseases; or refused to have induration or redness measurements recorded.

After the injection, skin color was compared among all participants using the Pantone International Standard Color Chart. Yellowness (Y) ranges from 1Y (neutral) to 5Y (most yellow), with higher values indicating greater saturation and a darker appearance. Redness (R) ranges from 1R (neutral) to 5R (pinkest), with higher values indicating greater saturation and a tendency to appear darker. Darker skin was defined as a vertical axis value ≥7 and a horizontal axis value of 1Y–6Y. A positive EC result was defined as an induration or redness reaction ≥5 mm.

Statistical Analysis

We used 2×2 contingency tables and means with standard deviations (SDs) to summarize continuous and categorical variables. The Fisher exact test or the χ^2 test was used for intergroup comparisons, as appropriate. Repeated-measures analysis of variance (ANOVA) was used to compare skin color and reaction time.

Latent mixture modeling in Stata software (version 16.0; College Station, Texas, US) identified distinct developmental trajectory groups within a population. Models with four, three, two, and one trajectory patterns were examined. The model with the smallest negative Bayesian Information Criterion (BIC) value was selected. Various functional forms were compared based on the significance levels of cubic, quadratic, and linear terms, with $P \leq 0.05$ considered statistically significant.

Ethical Approval and Participant Consent

This study received ethical approval from the human ethics committee of the Jiangsu Provincial Centers for Disease Control and Prevention was deemed necessary [approval number: JSJK2023-B029-02]. All eligible participants provided their consent by signing written informed consent forms.

RESULTS

Subject Characteristics

Ninety-six individuals from 40 countries across six continents participated in the study. Of the 96 international freshmen screened, 49 (51.04%) were female. The median age was 22 years [interquartile range (IQR), 19–27]. More than half (55.2%) were undergraduates. Additionally, 59 individuals (61.46%) originated from 15 countries with a high burden of tuberculosis. Moreover, 61 participants (63.5%) reported lighter skin (Table 1 and Figure 1).

Detection of *M. tb* Infection of Different Time

Supplementary Figure S1 (available at https://weekly.chinacdc.cn/) illustrates that, across all 96 individuals, induration diameters remained consistently smaller than corresponding redness diameters at 24, 48, 72, and 96 hours post-injection. After 24 hours, there were 3 positive cases (all related to redness), representing a 3.13% positivity rate. By 48 hours, positive cases increased to 7 (positivity rate: 7.29%), including 5

TABLE 1. Demographic characteristics of the 96 participants, overall and by trajectory patterns.

Variables	Trajectory patterns of ESAT6-CFP10 skin test			
	All	Continuous-increasing	Low-stable	Elevated-decreasing
N (%)	96 (100)	8 (8.3)	83 (86.5)	5 (5.2)
age	22 (19,27)	30 (19,35)	22 (19,27)	22 (21,30)
Sex				
Female	49 (51.0)	3 (37.5)	44 (53.0)	2 (40.0)
Male	47 (49.0)	5 (62.5)	39 (47.0)	3 (60.0)
Education				
Undergraduate	53 (55.2)	3 (37.5)	47 (56.6)	3 (60.0)
Postgraduate	43 (44.8)	5 (62.5)	36 (43.4)	2 (40.0)
Region				
Low-burden	37 (38.5)	3 (37.5)	32 (38.6)	2 (40.0)
High-burden	59 (61.5)	5 (62.5)	51 (61.4)	3 (60.0)
Skin color				
Lighter skin	61 (63.5)	3 (37.5)	53 (63.9)	5 (100.0)
Dark skin	35 (36.5)	5 (62.5)	30 (36.1)	0 (0)

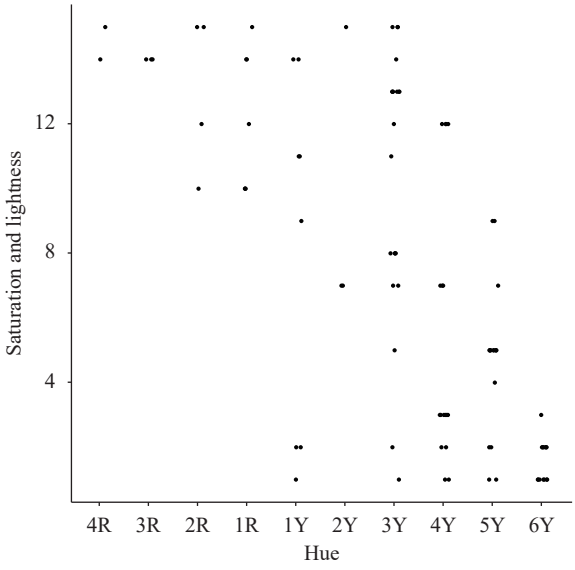

FIGURE 1. Scatter plot of skin color distribution among 96 students.
Note: Hue is a fundamental concept in color theory, representing the attribute of color that determines its name (such as red, blue, yellow, etc.). It is a primary dimension of color, used to describe the specific type of color. Horizontal axis (Y, yellowness) ranges from 1Y (neutral) to 5Y (most yellow), with higher values indicating increased saturation and a darker appearance. Vertical axis (R, redness) ranges from 1R (neutral) to 5R (pinkest), with higher values indicating greater saturation and a darker tone. Darker skin: defined by a vertical axis value of ≥7 and a horizontal axis value between 1Y and 6Y.

individuals from high-burden tuberculosis countries (71.43%). At 72 hours, positive cases rose to 13 (positivity rate: 13.54%), with 8 individuals originating from high-burden tuberculosis countries. The 96-hour assessment revealed 9 positive cases (positivity rate: 9.38%), with 6 from high-burden tuberculosis countries (66.67%).

Effects of Time and Skin Color on *M. tb* Infection

Table 2 displays results from repeated measures ANOVA for EC skin test time points. Analysis showed varying infection rates across time points, with the highest rate at 72 hours post-injection (F=5.310, *P*=0.001), regardless of skin color. *Mycobacterium tuberculosis* infection rates were lower among individuals with darker skin tones compared to those with lighter skin tones, although this difference was not statistically significant (*P*=0.186). These variations were not affected by different measurement times.

Trajectory Patterns of Different Measurement Time Points

Following the trajectory analysis, 8 individuals (5.3%) were classified into the continuous-increasing group, 83 individuals (86.5%) into the low-stable group, and 5 (5.2%) into the elevated-decreasing group (Figure 2). Notably, all individuals in the elevated-decreasing group had lighter skin tones, but trajectory patterns did not differ based on skin tone.

Safety of the EC Skin Test Among International Students

Two (2.1%) of the 96 international students in this study experienced adverse reactions during EC skin testing. One participant experienced dizziness, and the other exhibited hyperventilation. Symptoms in both cases were alleviated with symptomatic treatments, such as oxygen administration. No other severe adverse reactions were observed.

DISCUSSION

The Chinese government has prioritized tuberculosis prevention among students, emphasizing screening for close contacts and incoming freshmen. This proactive approach, outlined in national guidelines jointly formulated by the Ministry of Health and Ministry of

TABLE 2. Repeated measures ANOVA of different time results of EC skin test.

Test	Source	Type IV sum of squares	df	Mean square	F	*P*
Tests of within-subjects contrasts	Time	120.606	3	40.202	5.31	0.001
	Time*group	21.328	3	7.109	0.939	0.422
Tests of between-subjects effects	Intercept	557.644	1	557.644	6.411	0.013
	Color	154.532	1	154.532	1.777	0.186

Abbreviation: ANOVA=analysis of variance; EC=ESAT6-CFP10.

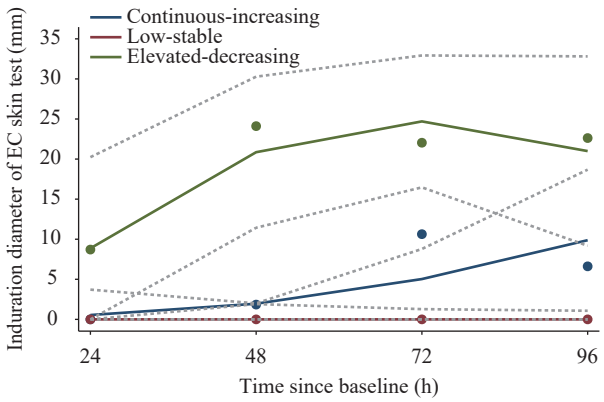

FIGURE 2. Trajectory patterns of latent tuberculosis infection over 24, 48, 72, and 96 hours in the screening cohort.

Education, demonstrates the government's commitment to student well-being (*3*). Despite this, the use of the EC skin test among foreign individuals with different skin tones, particularly recent immigrants from high-tuberculosis-incidence regions, remains unexplored in university settings, posing a potential gap in tuberculosis control efforts.

In China, the prevalence of *M. tb* infection is notably higher among foreign freshmen than among native freshmen. Studies in Shanghai and Beijing reported infection rates among freshmen using various tests: in Shanghai, rates were 3.45% with the EC skin test and 9.00% with the TST (*3*); in Beijing, among high school freshmen, rates were 9.10% with the EC skin test and 5.35% with the IGRA (*8*). An investigation in Chongqing revealed positive rates of 10.14% with the EC skin test and 24.13% with the TST. Another study in Jiangsu Province involving 26,398 students indicated a tuberculosis infection rate of 5.68% with the TST (*9*). However, infection rates among native Chinese students were consistently lower than those among foreign students. Elevated figures observed with the TST may be attributed to false positives associated with the Bacillus Calmette-Guérin vaccine (*10*).

In our study, we substantiated that the optimal timeframe for assessing the reaction to the EC skin test in foreign students is between 48 and 72 hours post-injection, aligning with the recommended instructions. This parallels the protocols of similar skin tests, such as Cy-Tb (Serum Institute of India, India) (*11*) and Diaskintest (Generium, Russian Federation) (*11*), which also advocate for the 48–72-hour window. Our research suggests that for evaluating the EC skin test in foreign students, 72 hours may be more appropriate than the commonly favored 48-hour mark. This conclusion is based on two randomized trials, which showed the highest median diameter of redness or induration at 48 hours compared to 24 and 72 hours. Interestingly, some foreign students initially had negative reactions at 48 hours but turned positive at 72 hours, with some showing increased reactivity up to 96 hours. The reasons for this phenomenon are unclear but could be due to darker skin tones requiring longer to show redness or delayed hypersensitivity among foreign students, necessitating a longer timeframe for reliable results (*12–13*).

In our study, we observed that the diameter of redness was consistently greater than that of induration among generally healthy foreign students (*7*), even when some reactions were positive at 24 h after injection. Notably, in contrast to Cy-Tb (Serum Institute of India, India) (*11*), Diaskintest (Generium, Russian Federation) (*14*), and TST (*15*), which rely on the measurement of induration diameter as the primary reaction parameter, our findings highlight the prevalence of a larger redness diameter in our participant cohort. One explanation is that the sensitivity of the skin test response was diminished by the removal of certain nonspecific antigens unrelated to *M. tb*. This modification may have reduced the test's ability to detect reactions effectively. Additionally, another factor influencing the observed differences is the distinct genetically modified bacillus used in the EC skin test compared to that used in Cy-Tb and Diaskintest (*5*).

Furthermore, our investigation revealed that skin color did not impact the response to the EC skin test. In contrast to Cy-Tb and Diaskintest, which measure induration, the EC skin test considers the greater measurement of either redness or induration. This might pose a challenge in accurately gauging reaction

diameter in individuals with darker skin tones. Notably, the diameter of redness was consistently larger than that of induration. Despite this observation, the finding that skin color does not influence the EC skin test response is reassuring and suggests its potential applicability for individuals with darker skin.

This study is subject to several limitations. First, the lack of a gold standard for *M. tb* infection precluded the use of IGRA or TST as a reference, limiting our ability to confirm the appropriateness of the 5mm cutoff point for the EC test in foreign individuals. Second, the small sample size limited our ability to determine the true *M. tb* infection rate among foreigners across subgroups. Future research should include larger studies of foreign individuals to comprehensively assess *M. tb* infection rates in diverse populations.

In summary, this study found a persistently high *M. tb* infection rate among foreign freshmen, as determined by the EC skin test. The test demonstrated a positive safety profile, with redness diameter proving a more reliable indicator than induration. It is recommended to assess EC skin test results between 48 and 72 hours, particularly if initial results at 24–48 hours are negative. Importantly, skin color did not impact test outcomes in our study. Greater attention should be given to international individuals, particularly recent immigrants from regions with high tuberculosis incidence, to address potential gaps in tuberculosis control efforts.

Conflicts of interest: No conflicts of interest.

Acknowledgements: The authors thank all investigators from the Jiangsu Provincial Center for Disease Control and Prevention and Nanjing Medical University.

Funding: Supported by Jiangsu Provincial Medical Key Discipline (ZDXK202250).

doi: 10.46234/ccdcw2024.191

[#] Corresponding authors: Limei Zhu, lilyam0921@163.com; Shiming Cheng, smcheng@163.com.

[1] Department of Chronic Communicable Disease, Jiangsu Provincial Center for Disease Control and Prevention, Nanjing City, Jiangsu Province, China; [2] Department of Epidemiology, School of Public Health, Nanjing Medical University, Nanjing City, Jiangsu Province, China; [3] Nanjing City Center for Disease Control and Prevention, Nanjing City, Jiangsu Province, China; [4] Chinese Antituberculosis Association, Beijing, China; [5] National Institutes for Food and Drug Control, Beijing, China.

[&] Joint first authors.

Submitted: March 31, 2024; Accepted: August 15, 2024

REFERENCES

1. Shah M, Dorman SE. Latent tuberculosis infection. N Engl J Med 2021;385(24):2271 – 80. https://doi.org/10.1056/NEJMcp2108501.
2. WHO. Guidelines on the management of latent tuberculosis infection. 2015. https://www.who.int/publications/i/item/9789241548908. [2015-1-1].
3. Huang W, Fang ZX, Luo S, Lin S, Xu L, Yan B, et al. The effect of BCG vaccination and risk factors for latent tuberculosis infection among college freshmen in China. Int J Infect Dis 2022;122:321 – 6. https://doi.org/10.1016/j.ijid.2022.06.010.
4. Su Q, Wang QY, Zhang T, Liu Y. Comparison of recombinant *Mycobacterium tuberculosis* fusion protein skin test and tuberculin skin test for screening latent tuberculosis infection in school students. Chin J Infect Control 2023;22(5):547 – 51. https://doi.org/10.12138/j.issn.1671-9638.20233724.
5. WHO. Rapid communication: TB antigen-based skin tests for the diagnosis of TB infection. 2022. https://www.who.int/publications/i/item/WHO-UCN-TB-2022.1. [2022-4-4].
6. Krutikov M, Faust L, Nikolayevskyy V, Hamada Y, Gupta RK, Cirillo D, et al. The diagnostic performance of novel skin-based in-vivo tests for tuberculosis infection compared with purified protein derivative tuberculin skin tests and blood-based in vitro interferon-γ release assays: a systematic review and meta-analysis. Lancet Infect Dis 2022;22(2):250 – 64. https://doi.org/10.1016/S1473-3099(21)00261-9.
7. Xu M, Lu W, Li T, Li JX, Du WX, Wu Q, et al. Sensitivity, specificity, and safety of a novel ESAT6-CFP10 skin test for tuberculosis infection in China: 2 randomized, self-controlled, parallel-group phase 2b trials. Clin Infect Dis 2022;74(4):668 – 77. https://doi.org/10.1093/cid/ciab472.
8. Yang Z, Sun Q, Han L, Bao C, Wang X, Zhang ZG. Analysis of recombinant mycobacterium tuberculosis fusion protein in screening for latent tuberculosis infection in college students. Chin J Front Med Sci (Electron Vers) 2022;14(7):51 – 4. https://doi.org/10.12037/YXQY.2022.07-10.
9. Wang WJ, Liu Q, Miao CD, Chen JJ, Wang Z, Zhu LM, et al. Status and influencing factors of latent tuberculosis infection among middle school students in Taizhou from 2019 to 2021. Chin J Dis Control Prev 2022;26(11):1264 – 70. https://doi.org/10.16462/j.cnki.zhjbkz.2022.11.005.
10. Gao L, Lu W, Bai LQ, Wang XH, Xu JS, Catanzaro A, et al. Latent tuberculosis infection in rural China: baseline results of a population-based, multicentre, prospective cohort study. Lancet Infect Dis 2015;15(3):310 – 9. https://doi.org/10.1016/S1473-3099(14)71085-0.
11. Ruhwald M, Aggerbeck H, Gallardo RV, Hoff ST, Villate JI, Borregaard B, et al. Safety and efficacy of the C-Tb skin test to diagnose *Mycobacterium tuberculosis* infection, compared with an interferon γ release assay and the tuberculin skin test: a phase 3, double-blind, randomised, controlled trial. Lancet Respir Med 2017;5(4):259 – 68. https://doi.org/10.1016/S2213-2600(16)30436-2.
12. Hauck FR, Neese BH, Panchal AS, El-Amin W. Identification and management of latent tuberculosis infection. Am Fam Physician 2009;79(10):879-86. https://www.aafp.org/pubs/afp/issues/2009/0515/p879.html.
13. Muñoz L, Stagg HR, Abubakar I. Diagnosis and management of latent tuberculosis infection. Cold Spring Harb Perspect Med 2015;5(11):a017830. https://doi.org/10.1101/cshperspect.a017830.
14. Nikitina IY, Karpina NL, Kasimceva OV, Gergert VY, Ergeshov A, Lyadova IV. Comparative performance of QuantiFERON-TB Gold versus skin test with tuberculosis recombinant allergen (Diaskintest) among patients with suspected pulmonary tuberculosis in Russia. Int J Infect Dis 2019;86:18 – 24. https://doi.org/10.1016/j.ijid.2019.06.014.
15. Kunst H. Diagnosis of latent tuberculosis infection: the potential role of new technologies. Respir Med 2006;100(12):2098 – 106. https://doi.org/10.1016/j.rmed.2006.02.032.

SUPPLEMENTARY MATERIAL

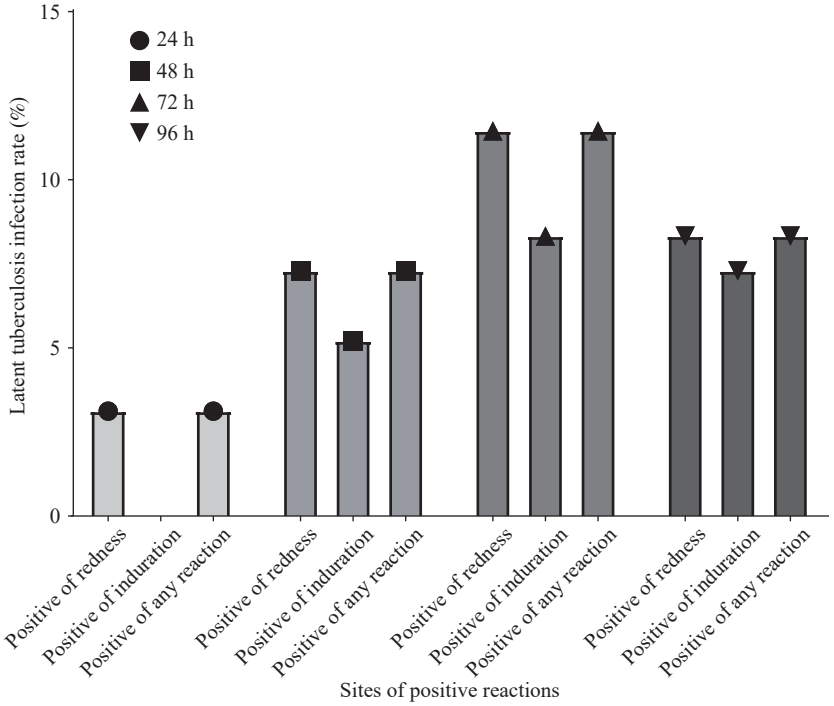

SUPPLEMENTARY FIGURE S1. Positive rates of redness and induration at 24, 48, 72, and 96 hours in the screening cohort.

Perspectives

The Implications of Artificial Intelligence on Infection Prevention and Control: Current Progress and Future Perspectives

Lin Yang[1]; Shuya Lu[1]; Lei Zhou[2,#]

The rapid advancement of artificial intelligence (AI) has significantly impacted infection prevention and control, particularly amid the coronavirus disease 2019 (COVID-19) pandemic (*1*). AI techniques such as machine learning (ML), deep learning, and natural language processing (NLP) have successfully transformed infection prevention and control strategies (*1*). These technologies have enhanced our understanding of infectious diseases, facilitated disease transmission prediction, and improved public health emergency responses (*2*). Despite these benefits, AI technologies encounter challenges related to ethics, biosafety, and privacy, including concerns about handling medical data by private entities and its potential misuse (*3–4*). Effectively utilizing AI in infection prevention and control requires balancing technical potential with ethical, policy, and societal considerations. In-depth research is essential to provide guidance for the responsible and effective use of AI technologies, thereby informing public health decision-makers and practitioners. This article discusses the current progress and future perspectives of AI applications in various aspects of infection prevention and control.

Disease Surveillance, Outbreak Prediction, and Contact Tracing

AI plays a crucial role in the surveillance and prediction of infectious disease outbreaks. Its ability to process diverse types of data allows healthcare authorities to take proactive measures. A notable example is the Canadian AI system, BlueDot, which uses NLP and ML to integrate various datasets and forecast different infectious diseases (*5–6*). By analyzing global aviation patterns, climate changes, zoonotic outbreaks, and epidemiological reports, BlueDot can provide earlier warnings compared to traditional surveillance networks. Additionally, it has been highly effective in projecting the spread of infections and identifying high-risk areas, thus informing public health policies and resource allocation. Numerous deep learning models have been developed to predict the antigenic evolution of various viruses, such as severe acute respiratory syndrome coronavirus 2 (SARS-CoV-2), influenza, human immunodeficiency virus (HIV), Lassa, and Nipah viruses (*7–8*). These achievements underscore the essential contribution of AI to global disease management frameworks.

The application of Bluetooth technology in contact tracing during the COVID-19 pandemic is illustrated by Singapore's TraceTogether app and Hong Kong Special Administrative Region (SAR), China's LeaveHomeSafe app (*9*). These applications facilitate the encrypted exchange of identifiers between nearby devices, with the data being securely stored on the users' devices. When a confirmed infection occurs, users can opt to share this data with health authorities, who can then notify potential contacts. A recent study in Hong Kong, China utilized Bluetooth technology for indoor positioning to develop a contact tracing system for high-risk areas such as schools and residential care homes (*10*). This method effectively manages contact tracing while respecting privacy, contributing significantly to the reduction of disease transmission in indoor settings. However, concerns about data security and personal privacy present obstacles to maintaining user compliance with these tracing systems, which require access to personal mobile devices. Additionally, integrating both indoor and outdoor contact tracing into a single platform remains a challenge.

Diagnosis and Treatment

During the initial phase of the COVID-19 pandemic, AI significantly improved the efficiency of diagnosing early-stage COVID-19 infections, particularly through the autonomous analysis of chest X-ray images (*11*). AI algorithms demonstrated the capability to rapidly diagnose COVID-19 even when radiological findings appeared normal by integrating clinical symptoms, exposure history, and laboratory

tests (*12*). Deep learning methods have also been widely applied to identify other infectious diseases, including tuberculosis (*13*) and hepatic echinococcosis (*14*). AI-powered image analysis tools exhibit impressive sensitivity and precision, showing significant potential for disease screening in under-resourced areas with limited healthcare facilities.

DeepMind's AlphaFold algorithm has significantly advanced the decoding of protein structures for SARS-CoV-2 and vaccine development (*15*). Traditional techniques like X-ray crystallography and cryo-electron microscopy are both labor-intensive and time-consuming. In contrast, AlphaFold employs a convolutional neural network trained on Protein Data Bank data to accurately predict protein structures. This algorithm has been widely adopted in the identification of drug candidates for cancer, Alzheimer's disease, and vaccine development (*16*).

Pandemic Preparedness and Response

During the pandemic, AI techniques can be utilized for epidemic forecasting, resource management, and information dissemination to alleviate pressure on hospitals (*17*). A study conducted in Hong Kong SAR, China, utilized deep reinforcement learning (DRL) to analyze diverse data, including travel behaviors, climatic variations, and social media trends. The study aimed to develop adaptive non-pharmacological interventions (NPIs) for managing COVID-19 and other respiratory infectious diseases (*18*). These interventions effectively contained disease outbreaks within the capacity constraints of healthcare systems. The DRL approach strategically controlled the trajectory of the outbreaks, ensuring they remained close to full capacity limits. This strategy expedited the achievement of herd immunity while minimizing resource utilization.

Furthermore, AI has significantly contributed to the effective dissemination of disease prevention and control information. A notable example is the AI-powered chatbot developed by the World Health Organization, which provided reliable information and helped alleviate public anxiety during the pandemic (*19*). Additionally, AI has been crucial in monitoring social media platforms to identify and address COVID-19 misinformation, thereby reducing the spread of rumors (*20*). For instance, NLP methods have been employed to conduct sentiment analysis on posts from Twitter and Reddit, aiming to identify negative communications and misinformation related to COVID-19 (*21*).

Ethical and Safety Concerns

The growing application of AI in medicine and public health underscores its crucial role in enhancing disease surveillance, early detection of infectious diseases, resource allocation, and crisis management. Nevertheless, this expansion also raises significant ethical and safety concerns.

The application of AI in vaccine development raises ethical issues related to data privacy, bias, and equity. AI is widely used to analyze data, including personal health records and genetic information, which underscores the necessity of protecting data privacy. Furthermore, the uneven distribution of healthcare resources leads to biased data in vaccine development, often favoring populations with greater healthcare access (*22*). This imbalance, combined with potential biases, can result in vaccines being less effective and safe for various populations. On a national level, this disparity can exacerbate differences in healthcare standards between developed and developing countries. Therefore, it is essential to use AI ethically in vaccine development to ensure that populations with limited healthcare access also benefit from emerging technologies and to reduce global health disparities.

Without adequate regulation and oversight, the use of AI in vaccine development and distribution may present significant ethical and safety concerns. To address these issues, international legislative efforts, such as those led by the WHO, as well as initiatives in countries like the United States and the United Kingdom, have been implemented (*23*).

The rapid dissemination of information facilitated by AI has inadvertently contributed to the spread of misinformation, particularly during the COVID-19 pandemic. This misinformation poses substantial challenges to epidemic prevention and control. One study conducted a large-scale observational analysis of 76,985 Twitter (now known as X) users, examining over 80 million posts published over 18.5 months (*24*). The findings indicated that individuals who shared COVID-19 misinformation experienced approximately twice the level of anxiety compared to those who did not spread misinformation, resulting in significant adverse psychological effects. These results underscore the psychological impact of misinformation on public mental health and emphasize the need to enhance public discernment of information sources and enforce robust regulation of social media and online platforms. In response, China has reinforced its regulations to protect data security and personal

privacy. This includes the 2021 implementation of the "Cybersecurity Law," "Data Security Law" (DSL), and "Personal Information Protection Law" (PIPL) (*25–27*).

In summary, recent advancements in AI, particularly in generative AI models, have significantly impacted various industries. AI has been crucial in predicting epidemics and optimizing resource allocation during the pandemic. It has revolutionized drug design and disease management by providing fast and accurate predictions for diagnosis, disease progression, and treatment development. AI is expected to play an increasingly important role in managing future public health emergencies, particularly in addressing infectious disease outbreaks (*28–29*). However, it is essential to address the ethical and safety concerns that accompany this growth. The recent breakthroughs in generative AI, such as OpenAI's ChatGPT and video generation tools like SORA, offer significant opportunities for interactive and personalized health education. Nevertheless, the potential for misinformation through hallucinations and fake videos poses a risk of disseminating false information, thereby undermining efforts to combat infectious diseases.

To effectively address these challenges, it is crucial to establish international collaboration, enforce strict regulations, maintain ethical oversight, and improve public information literacy. These measures are essential for maximizing the benefits of AI while mitigating associated risks. The successful realization of AI's transformative impact on human civilization depends on a unified effort from global public health organizations, research institutions, and scientists, all focused on promoting universal human welfare (*2*). Regulators should continuously assess and manage the ethical and safety concerns associated with the use of AI in infection prevention and control. Policymakers must proactively address future challenges by enacting laws and regulations that guarantee information security and uphold medical ethics. This approach will foster a conducive environment for the stable development of AI.

Conflicts of interests: No conflicts of interest.

Funding: Supported by the National Natural Science Foundation Project of the People's Republic of China (grant number: 71934002); and the Health and Medical Research Fund (HMRF) commissioned studies on COVID-19 research (reference number COVID1903007).

doi: 10.46234/ccdcw2024.192

[#] Corresponding author: Lei Zhou, zhoulei@chinacdc.cn.

[1] School of Nursing, The Hong Kong Polytechnic University, Hong Kong Special Administrative Region, China; [2] Chinese Center for Disease Control and Prevention, Beijing, China.

Submitted: April 12, 2024; Accepted: July 16, 2024

REFERENCES

1. Syrowatka A, Kuznetsova M, Alsubai A, Beckman AL, Bain PA, Craig KJT, et al. Leveraging artificial intelligence for pandemic preparedness and response: a scoping review to identify key use cases. npj Digit Med 2021;4(1):96. https://doi.org/10.1038/s41746-021-00459-8.
2. Jia ZW, Yan XY, Li YJ, Ma JQ. Internet data for improving prevention and control of global infectious diseases. China CDC Wkly 2020;2(52): 1009 – 12. https://doi.org/10.46234/ccdcw2020.269.
3. Bélisle-Pipon JC, Vayena E, Green RC, Cohen IG. Genetic testing, insurance discrimination and medical research: what the United States can learn from peer countries. Nat Med 2019;25(8):1198 – 204. https://doi.org/10.1038/s41591-019-0534-z.
4. Wan ZY, Hazel JW, Clayton EW, Vorobeychik Y, Kantarcioglu M, Malin BA. Sociotechnical safeguards for genomic data privacy. Nat Rev Genet 2022;23(7):429 – 45. https://doi.org/10.1038/s41576-022-00455-y.
5. Bogoch II, Watts A, Thomas-Bachli A, Huber C, Kraemer MUG, Khan K. Pneumonia of unknown aetiology in Wuhan, China: potential for international spread via commercial air travel. J Travel Med 2020;27(2): taaa008. https://doi.org/10.1093/jtm/taaa008.
6. Bluedot: Outbreak Intelligence Platform [Internet]. Bluedot. 2022. https://bluedot.global/. [2024-1-21].
7. Han WK, Chen NN, Xu XZ, Sahil A, Zhou JX, Li ZX, et al. Predicting the antigenic evolution of SARS-COV-2 with deep learning. Nat Commun 2023;14(1):3478. https://doi.org/10.1038/s41467-023-39199-6.
8. Thadani NN, Gurev S, Notin P, Youssef N, Rollins NJ, Ritter D, et al. Learning from prepandemic data to forecast viral escape. Nature 2023;622(7984):818 – 25. https://doi.org/10.1038/s41586-023-06617-0.
9. Stevens H, Haines MB. Tracetogether: pandemic response, democracy, and technology. East Asian Sci, Technol Soc: Int J 2020;14(3):523 – 32. https://doi.org/10.1215/18752160-8698301.
10. Meng JH, Liu JYW, Yang L, Wong MS, Tsang H, Yu BY, et al. An AI-empowered indoor digital contact tracing system for COVID-19 outbreaks in residential care homes. Infect Dis Modell 2024;9(2):474 – 82. https://doi.org/10.1016/j.idm.2024.02.002.
11. Wang LD, Lin ZQ, Wong A. COVID-Net: A tailored deep convolutional neural network design for detection of covid-19 cases from chest x-ray images. Sci Rep 2020;10(1):19549. https://doi.org/10.1038/s41598-020-76550-z.
12. Mei XY, Lee HC, Diao KY, Huang MQ, Lin B, Liu CY, et al. Artificial intelligence–enabled rapid diagnosis of patients with COVID-19. Nat Med 2020;26(8):1224 – 8. https://doi.org/10.1038/s41591-020-0931-3.
13. Huang CX, Wang W, Zhang X, Wang SH, Zhang YD. Tuberculosis diagnosis using deep transferred EfficientNet. IEEE/ACM Trans Comput Biol Bioinf 2023;20(5):2639 – 46. https://doi.org/10.1109/TCBB.2022.3199572.
14. Wang Z, Bian HY, Li JQ, Xu J, Fan HN, Wu XZ, et al. Detection and subtyping of hepatic echinococcosis from plain CT images with deep learning: a retrospective, multicentre study. Lancet Digital Health 2023;5(11):e754 – 62. https://doi.org/10.1016/s2589-7500(23)00136-x.
15. Thornton JM, Laskowski RA, Borkakoti N. AlphaFold heralds a data-driven revolution in biology and medicine. Nat Med 2021;27(10): 1666 – 9. https://doi.org/10.1038/s41591-021-01533-0.
16. Ren F, Ding X, Zheng M, Korzinkin M, Cai X, Zhu W, et al. AlphaFold accelerates artificial intelligence powered drug discovery: efficient discovery of a novel CDK20 small molecule inhibitor. Chem

Sci 2023;14(6):1443 – 52. https://doi.org/10.1039/d2sc05709c.
17. Lin TF, Zhao ZY, Yang ZR, Li BL, Wei C, Li FX, et al. Hospital strain and COVID-19 fatality—England, April 2020–March 2022. China CDC Wkly 2022;4(52):1176 – 80. https://doi.org/10.46234/ccdcw2022.236.
18. Yao Y, Zhou HC, Cao ZD, Zeng DD, Zhang QP. Optimal adaptive nonpharmaceutical interventions to mitigate the outbreak of respiratory infections following the COVID-19 pandemic: a deep reinforcement learning study in Hong Kong, China. J Am Med Inform Assoc 2023;30(9):1543 – 51. https://doi.org/10.1093/jamia/ocad116.
19. Miner AS, Laranjo L, Kocaballi AB. Chatbots in the fight against the COVID-19 pandemic. npj Digit Med 2020;3(1):65. https://doi.org/10.1038/s41746-020-0280-0.
20. Lin J, Nogueira R, Yates A. Pretrained transformers for text ranking: Bert and beyond [M]. Springer Nature, 2022.
21. Arbane M, Benlamri R, Brik Y, Alahmar AD. Social media-based COVID-19 sentiment classification model using Bi-LSTM. Expert Syst Appl 2023;212:118710. https://doi.org/10.1016/j.eswa.2022.118710.
22. Smith J, Lipsitch M, Almond JW. Vaccine production, distribution, access, and uptake. Lancet 2011;378(9789):428 – 38. https://doi.org/10.1016/S0140-6736(11)60478-9.
23. WHO. WHO issues first global report on Artificial Intelligence (AI) in health and six guiding principles for its design and use. World Health Organization. 2021. https://www.who.int/news/item/28-06-2021-who-issues-first-global-report-on-ai-in-health-and-six-guiding-principles-for-its-design-and-use. [2024-1-21].
24. Verma G, Bhardwaj A, Aledavood T, De Choudhury M, Kumar S. Examining the impact of sharing COVID-19 misinformation online on mental health. Sci Rep 2022;12(1):8045. https://doi.org/10.1038/s41598-022-11488-y.
25. China PsRo. Cybersecurity law of the People's Republic of China. Beijing: National People's Congress; 2017. https://www.gov.cn/xinwen/2016-11/07/content_5129723.htm. [2024-1-21]. (In Chinese).
26. China PsRo. Data security law of the People's Republic of China. Beijing: National People's Congress; 2021. https://www.gov.cn/xinwen/2021-06/11/content_5616919.htm. [2024-1-21]. (In Chinese).
27. China PsRo. Personal information protection law of the People's Republic of China. Beijing: National People's Congress; 2021. https://www.gov.cn/xinwen/2021-08/20/content_5632486.htm. [2024-1-21]. (In Chinese).
28. Brownstein JS, Rader B, Astley CM, Tian HY. Advances in artificial intelligence for infectious-disease surveillance. N Engl J Med 2023;388(17):1597 – 607. https://doi.org/10.1056/nejmra2119215.
29. Wong F, De La Fuente-Nunez C, Collins JJ. Leveraging artificial intelligence in the fight against infectious diseases. Science 2023;381(6654):164 – 70. https://doi.org/10.1126/science.adh1114.

Youth Editorial Board

Indexed by Science Citation Index Expanded (SCIE), Social Sciences Citation Index (SSCI), PubMed Central (PMC), Scopus, Chinese Scientific and Technical Papers and Citations, and Chinese Science Citation Database (CSCD)

The inauguration of *China CDC Weekly* is in part supported by Project for Enhancing International Impact of China STM Journals Category D (PIIJ2-D-04-(2018)) of China Association for Science and Technology (CAST).

CCDC weekly

Vol. 6 No. 35 Aug. 30, 2024

Responsible Authority
National Disease Control and Prevention Administration

Sponsor
Chinese Center for Disease Control and Prevention

Editing and Publishing
China CDC Weekly Editorial Office
No.155 Changbai Road, Changping District, Beijing, China
Tel: 86-10-63150501, 63150701
Email: weekly@chinacdc.cn

CSSN
ISSN 2096-7071 (Print)
ISSN 2096-3101 (Online)
CN 10-1629/R1